

## Pseudocrystalline model of the magnetic anisotropy in amorphous rare-earth–transition-metal thin films

D. Mergel

*Philips Research Laboratories Aachen, Weisshausstrasse, D-5100 Aachen, Germany*

H. Heitmann

*Fachhochschule Wedel, Feldstrasse 143, D-2000 Wedel/Holstein, Germany*

P. Hansen

*Philips Research Laboratories Aachen, Weisshausstrasse, D-5100 Aachen, Germany*

(Received 2 July 1992; revised manuscript received 14 September 1992)

A pseudocrystalline model is proposed to explain the occurrence of perpendicular anisotropy in amorphous rare-earth–transition metal (*R-T*) thin films. It is based on the central hypothesis that during layer-by-layer growth small planar hexagonal units are formed defining on average a preferential axis perpendicular to the film plane. The units are similar in structure to relaxed crystalline ones and are estimated to typically comprise six rare-earth atoms. They are regarded as an idealized model of the short-range order and are consistent with the known nearest-neighbor *R-T* and *T-T* coordination numbers in the amorphous state. This model is able to explain the known experimental results concerning the influence of composition, substrate temperature, annealing, and bombardment effects during sputter deposition on the magnetic anisotropy of thin amorphous rare-earth–transition-metal films of the system (Nd, Tb, Dy) (Fe, Co), as well as the destruction of this anisotropy by additives.

### I. INTRODUCTION

Amorphous thin films consisting of rare-earth–transition-metal (*R-T*) alloys were prepared in 1972 by coevaporation of Gd and Fe in the compositional range 15–94 at % Fe.<sup>1</sup> In 1973 it was discovered that sputtered Gd-Co and Gd-Fe films contain stripe and cylindrical domains indicating perpendicular anisotropy, and it was demonstrated that these films are suited as media for magneto-optic (MO) recording.<sup>2</sup> Since that time the magnetic properties of *R-T* amorphous thin films have been intensively studied, and MO recording using *R-T* media has been developed into a mature technology which is now being introduced into the market.

In order to explain the perpendicular magnetic anisotropy in amorphous *R-T* thin films several mechanisms have been proposed. However, there is no satisfactory and consistent explanation of the major experimental results by only one of these mechanisms and consequently there is no agreement in the literature on the acceptance of one or the other model. For a recent discussion see, e.g., Refs. 3 and 4.

There should be no macroscopic magnetic anisotropy in an ideal amorphous structure. Therefore, a macroscopic magnetic anisotropy presupposes a structural anisotropy at least on an atomic level or on a nanometer scale. In addition, there must be a magnetic interaction with the anisotropic structure.

The magnetic interactions can be dipolar interactions between neighboring magnetic moments, spin-orbit coupling, or magnetostriction. For materials with axial symmetry, dipole interactions have to be considered. For non-*S* state ions (e.g., Tb, Dy, Ho, . . .), spin-orbit cou-

pling generally is the most important interaction resulting in single-ion anisotropy or anisotropic exchange, giving rise to anisotropies which are generally at least one order of magnitude larger than that caused by dipole effects. This can be seen comparing Gd (*S* state) -Fe,Co and Tb (non-*S*) -Fe,Co alloys.<sup>5</sup>

We presuppose that a single-ion mechanism is predominant for non-*S*-state rare-earth-containing alloys [e.g., (Nd,Tb,Dy) (Fe,Co)] as has already been proposed by several authors. The case of Gd-(Fe,Co) can be more complicated because here several effects of the same order of magnitude can simultaneously act and even compensate each other.

In this paper we suggest an explanation for the structural anisotropy that is based on the often observed tendency that in amorphous matter the short-range order of the crystalline structure is preserved.<sup>6</sup> The apparent difference between the amorphous and the crystalline structures concerns the disappearance of long-range order. The starting point of our discussion is the fact that for the technologically relevant compositional range there are crystalline counterparts the structure of which originates from the hexagonal lattice of the CaCu<sub>2</sub> type. Our hypothesis is that also in the “amorphous” state crystallinelike environments are preserved (“pseudocrystalline units”) and are the origin of the perpendicular anisotropy.

We define our pseudocrystalline model in Sec. II, and in Sec. III we try to interpret the experimental results concerning the parameters of preparation and composition that have revealed an influence on the perpendicular anisotropy. The models presented so far in the literature, such as magnetoelastic interactions, inhomogeneous

structure, bombardment-induced, and microcrystallites are discussed with respect to our model in Sec. IV with special emphasis on bond-orientational anisotropy<sup>3</sup> and growth-induced texturing.<sup>4</sup> Finally, some recommendations and suggestions for future investigations are made.

## II. PSEUDOCRYSTALLINE MODEL

For the technologically relevant compositions of the amorphous layers there are crystalline counterparts the structure of which originates from the hexagonal lattice of the  $\text{CaCu}_5$  type.<sup>7-9</sup> For  $RT_5$  this structure consists of a stacking of double layers where one layer has the chemical composition  $RT_2$  and the other one contains only  $T$  atoms as sketched in Fig. 1. For  $RT_2$  the stacking unit consists of three layers as shown in Fig. 2. For compounds between these two intermetallics (e.g.,  $R_2T_7, RT_3$ ) both types of layers are present.

For the amorphous structure we suggest a relaxation in the  $T$  plane as indicated in Fig. 1 by arrows, making crystalline second-nearest  $T$ - $R$  neighbors to (approximately) nearest neighbors. This relaxed structure is in agreement with the coordination numbers found in structural investigations of amorphous Tb-Fe summarized in Table I (compiled from Refs. 10-13). For  $T$ - $T$  pairs, coordination numbers between 6.8 and 9.1 are found. Our relaxed structure can explain coordination numbers between 6 and 8, with each three  $T$  neighbors in the  $T$  planes above and below the  $R$ -containing plane plus one  $T$  centrally above, and another one from the next bilayer below (compare Fig. 1). For  $R$ - $T$  pairs the experimentally found coordination numbers are 10.7-13.3. In our relaxed structure we would expect values around 12 (six neighbors in the  $R$ -containing plane, three in each of the adjacent  $T$  planes). For  $R$ - $R$  pairs, coordination numbers between 0 and 3.9 are found, while in our model a coordination number of zero is predicted.

Thin-film growth is known to occur layer by layer.<sup>14</sup> The starting hypothesis of our model is that, during this layer-by-layer growth, small pseudocrystalline planar configurations of the type of Figs. 1 and 2 are formed with an average alignment of the axis parallel to the film normal and stacked so that some crystalline short-range order is preserved, but no long-range order is involved. The main characteristics of this model are that it is

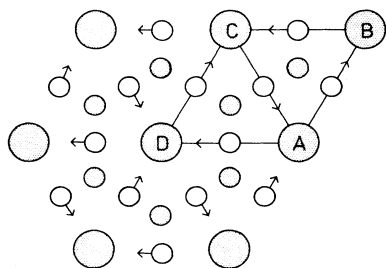


FIG. 1. Planes of  $RT_5$  intermetallic compounds. Different shading designates different planes.  $ABCD$  denotes the unit cell. Circles with the larger radius represent  $R$  atoms. The atoms in the  $T$  plane are supposed to relax in the amorphous state with respect to the crystalline state as indicated by arrows.

atomistic but involves a structure that extends over more than nearest neighbors and is similar to the energetically minimal crystalline configuration so that it is thermodynamically favored. The pseudocrystallinity is supposed to be a purely local structural effect and not viewed as truly nanocrystalline.

The proposed relaxed structure of  $T$  atoms in the  $T$  plane causes additional anisotropic electrostatic fields at  $R$  sites with an average component perpendicular to the film plane leading via spin-orbit coupling to a perpendicular magnetic anisotropy.

We would expect that such a pseudocrystalline structure with an average preferential axis perpendicular to the plane will yield an anisotropic distribution of nearest-neighbor distances with denser in-plane packing as was observed by small-angle x-ray scattering.<sup>3</sup>

The polarization dependence of extended x-ray-absorption fine structure has been employed to investigate the atomic structure parallel and perpendicular to the film plane of a series of  $\text{Tb}_{1-x}\text{Fe}_x$  amorphous films with  $x = 0.74-0.84$ .<sup>15</sup> Quantitative modeling shows that the observed structural anisotropy can be described as anisotropic near-neighbor pair correlations, with Tb-Tb and Fe-Fe pair correlations greater in plane and Fe-Tb greater perpendicular to the film plane. These findings support our layered pseudocrystalline model.

Our model is idealized. In reality the hexagonal units may not really be formed homogeneously, but a tendency toward formation is supported by the energetically minimal configuration in the crystalline structure and the layer-by-layer growth.

## III. INTERPRETATION OF EXPERIMENTAL RESULTS

Many parameters have revealed an influence on the perpendicular magnetic anisotropy in amorphous  $R$ - $T$  films. The most prominent influences are due to composition, additives, substrate temperature during preparation, bombardment effects during sputter deposition, and annealing. They have been partly discussed and interpreted within the existing models. In this section we strive to get an overview of major experiments reported in the literature, with a critical discussion of the experimental conditions, and to interpret them on the basis of the pseudocrystalline model.

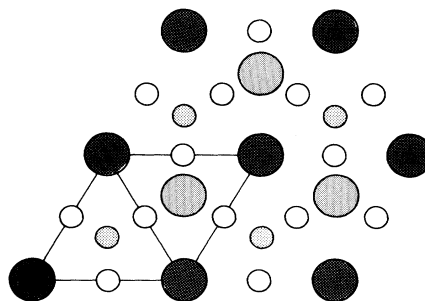


FIG. 2. Planes of  $RT_2$  intermetallic compounds. Different shading designates different planes. Circles with the larger radius represent  $R$  atoms.

TABLE I. Coordination numbers  $c$  and average interatomic distances  $r$  (in Å) of amorphous  $R$ - $T$  films.

	$r_{T-T}$	$c_{T-T}$	$r_{R-T}$	$c_{R-T}$	$r_{R-R}$	$c_{R-R}$	Ref.
Tb <sub>21</sub> Fe <sub>79</sub>	2.59	7.0	3.06		3.49	6.9	10
Tb <sub>19</sub> Fe <sub>81</sub>	2.52	6.8	3.02	12.3	3.41	3.9	11
24-h anneal	2.55	8.4	3.08	12.3	3.50	3.5	
Tb <sub>19</sub> Co <sub>81</sub>	2.48	7.3	2.95	12.5	3.36	3.6	11
24-h anneal	2.48	7.3	2.99	13.3	3.41	3.1	
Tb <sub>20</sub> Fe <sub>80</sub>	2.50	9.1±1	2.94	10.7		0	12
Annealed	2.50	9.5	2.95	12.6			
Tb <sub>1-x</sub> Fe <sub>x</sub> , x = 0.16–0.23							13
1. Shell	2.47	4.5–5.0	(2.43 Oxygen)				
2. Shell	2.66	2.5–3.0	2.91	9.5±1	3.4	3.5±1	
Sum		7.0–8.0					

### A. Compositional dependence

Maxima in the compositional dependence of the perpendicular magnetic anisotropy are found for different binary systems of transition metals and heavy or light rare-earth elements. E.g., for electron-beam-evaporated films a maximum at 20 at % Tb for Tb-Fe,<sup>16</sup> a maximum at 30–40 at % Dy for Dy-Fe,<sup>17</sup> and a maximum at 25 at % Dy for Dy-Co (Refs. 18 and 17) were observed. Also, for cosputtered Tb-Fe, a maximum at 20 at % Tb is reported.<sup>19</sup> For more than 50 at % heavy  $R$ , generally an in-plane anisotropy is observed. For Nd-Fe (Refs. 16 and 20) and Pr-Fe,<sup>16</sup> a maximum at 40 at % light  $R$  and for Nd-Co (Refs. 17 and 21) and Pr-Co,<sup>17</sup> a maximum at 22 at % light  $R$  are found.

Some results of  $K_u$  at 77 K are displayed in Fig. 3 for the system  $R_{1-x}T_x$  with  $R = \text{Nd, Dy}$  and  $T = \text{Fe, Co}$ . The technologically relevant Tb-based compositions are difficult to measure because of their high coercivity, therefore only data for Tb-Fe at 300 K measuring temperature are incorporated in Fig. 3.

When interpreting these data, one has to take into account that the Curie temperature  $T_C$  of the binary amorphous alloys exhibit a strong dependence on composition, affecting the observed compositional dependence of  $K_u$  at measuring temperatures not far enough away from the Curie temperature. Therefore it could be argued that the observed dependence of  $K_u$  can be caused by this  $T_C$  variation.

This argument is especially important for Fe-based alloys which exhibit a maximum in the Curie temperature (e.g.,  $T_{C\text{max}} = 400$  K for Tb-Fe) for this range of compositions. A maximum of  $K_u(x)$  occurs, however, also for Co-based alloys for which the magnetic coupling is much less sensitive to structural effects and, in particular, the Curie temperature shows no maximum at a certain composition but increases almost continuously between the minimum at the critical composition (about 50 at % Co) and the Curie temperature of crystalline Co (1388 K).<sup>24,25</sup> Therefore the decrease of  $K_u$  with increasing Co content on the  $T$ -rich side is not caused by a Curie temperature effect.

The influence of  $T_C$  on  $K_u$  can be estimated from Fig.

3 where those compositions are indicated on the  $K_u = 0$  axis at which  $T_C$  is equal to the measuring temperature and therefore zero magnetic anisotropy is expected *a priori*. The influence of  $T_C$  on  $K_u$  can be strong in the cases of Nd-Fe and Tb-Fe, in the latter case only on the  $T$ -rich side. For the other systems where also a compositional maximum is observed at 77 K, this influence is significantly reduced and the direct compositional dependence should be predominant.

Altogether we conclude that the observed maxima of  $K_u$  for Dy-Fe, Dy-Co, and Nd-Co are directly related to

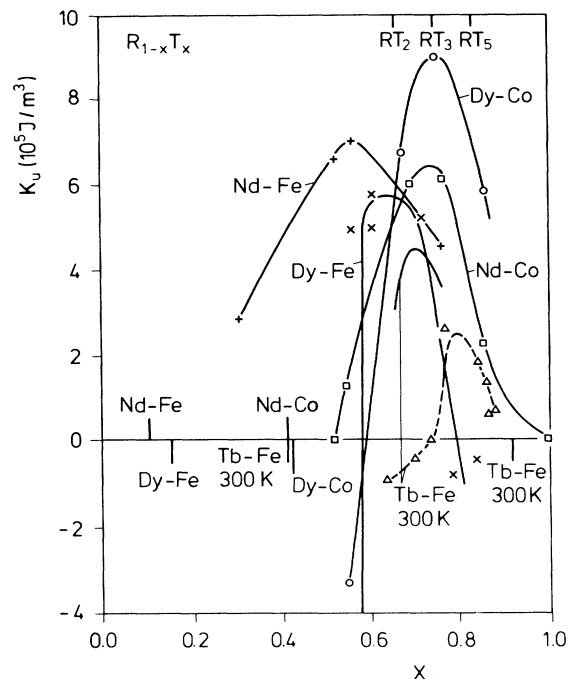


FIG. 3. Compositional dependence of  $K_u$ . In order to estimate an indirect effect of the Curie temperature on  $K_u$  those compositions are indicated on the  $x$  axis for which the Curie temperature is equal to the measuring temperature. Nd-T (Ref. 22), Tb-Fe (— — —): deposited at 77 K (Ref. 19), (—): deposited at 300 K, (Ref. 23) Dy-Fe (Ref. 16), Dy-Co (Ref. 17).

the composition. Nd-Fe (and also Pr-Fe) is a special case in that the maximum in  $K_u(x)$  cannot be attributed directly to the composition because indirect effects due to the Curie temperature dependence  $T_C(x)$  cannot be ruled out.

We now try to relate the compositional dependence of  $K_u$  to the structure and magnetic anisotropy of the crystalline counterparts. A survey of the crystal structures of binary  $R$ - $T$  intermetallics originating from the  $\text{CaCu}_5$  type together with their magnetic easy axis is given in Table II (compiled from Refs. 9 and 25).

The  $R$ -rich crystalline compounds  $RT_2$  are cubic and consequently have no singular easy magnetic axis. The crystalline compounds of higher transition-metal content have axial structures, with the exception of  $R_6\text{Fe}_{23}$ . The Co-based intermetallics exhibit an easy axis which is the  $c$  axis perpendicular to the basal plane. On the contrary, the Fe-based compounds have their easy axis in the basal plane. In a first trial one would therefore expect that Fe-based amorphous films exhibit an in-plane anisotropy. We assume that the relaxation of Fe atoms in the  $T$  plane that causes a stronger average electrostatic field perpendicular to the film plane is the reason for the occurrence of perpendicular magnetic anisotropy also in Fe-based amorphous alloys.

The relaxation leads locally to an  $R$ - $T$  configuration similar to that at an interface between an  $R$  and a  $T$  layer. The assumption made above is therefore supported by the fact that in superlattices consisting of alternating layers of Tb and Fe also a strong perpendicular anisotropy is found and attributed to Tb-Fe interactions across the interface.<sup>26-29</sup>

In the amorphous case a maximum is expected for a composition where the maximum number of hexagonal units is formed during thin-film growth. On the  $T$ -rich side we come from the low anisotropy of amorphous Fe or Co, and the increase of  $K_u$  with increasing Tb or Dy content can be understood in terms of single-ion behavior together with a tendency to form the pseudocrystalline axial environments. On the  $R$ -rich side beyond  $RT_2$  there should be a tendency to form cubic environments corresponding to the crystalline counterparts leading to a decrease in  $K_u$ . This structural explanation is also supported by the exceptional behavior of Nd-Fe which forms no crystalline cubic intermetallics and exhibits perpendicular magnetic anisotropy in the amorphous state over the

whole compositional range.

The maximum  $K_u$  values in amorphous thin films are considerably smaller than typical crystalline anisotropy constants<sup>9</sup> (e.g.,  $K_1=2\times 10^6$  J/m<sup>3</sup> for  $\text{DyFe}_2$  and  $K_1=-6.3\times 10^6$  J/m<sup>3</sup> for  $\text{TbFe}_2$ ) except for Nd-Co ( $K_1=7\times 10^5$  J/m<sup>3</sup> for  $\text{NdCo}_5$ ), where comparable values are reached.

### B. Destruction of $K_u$ by additives

In the literature no increase of  $K_u$  due to "nonmagnetic" additives but mostly strong destructive effects have been reported. In Table III (compiled from Refs. 30-36) the effects of several additives have been summarized.

With respect to their effect on  $K_u$ , a distinction between additives with a metallic bond and those with covalent bonds has to be made.

For metallic additives at concentrations up to 20 at. % in the system (Tb,Gd)-(Fe,Co) the anisotropy is still perpendicular. The ratio of Tb to Gd and the ratio of Fe to Co seem to play no role. Beryllium is an exception because even alloys with a content of 40 at. % Be still show a perpendicular anisotropy. The obvious reason is that Be atoms with their small atomic radii fit well into the gaps of the amorphous structure without disturbing it. Additive atoms with metal bonding to rare-earth elements will take the same sites as the  $T$  atoms and will therefore not destroy the local structure. Consequently, the magnetic properties reduce slowly, linearly with increasing additive content.

For covalently bonded additives, e.g., Si, Ge, N, and especially for oxygen ("reactive additives"),  $K_u$  becomes negative (in-plane magnetization) at much lower concentration: 2-8 at. %, corresponding to typically one additive atom per 12 to 3  $R$  atoms.

This effect on  $K_u$  is much stronger than the effects on the magnetic system characterized by the compensation and Curie temperatures which are listed in Table I for comparison. The most pronounced effect on the compensation temperature  $T_{\text{comp}}$  is observed for oxygen additions. A content of 1 at. % oxygen shifts  $T_{\text{comp}}$  by up to 120 K, corresponding in effect to a decrease of the Gd content also by approximately 1 at. %. This is an indication that one oxygen atom eliminates one  $R$  atom from the magnetic matrix. The metallic additives lead to a rel-

TABLE II. Crystal structure of intermetallic  $R$ - $T$  compounds and their easy magnetic axis (compiled from Ref. 9, data for Gd-Co from Ref. 25).

$R$ -Co	$R$ -Fe	$R$ -Co	$R$ -Fe	$R$ -Co	$R$ -Fe	$R$ -Co	$R$ -Fe
Cubic	Cubic	Rhom	Rhom	Hex	Cubic	Hex	Rhom
NdCo <sub>2</sub>		NdCo <sub>3</sub>		Nd <sub>2</sub> Co <sub>7</sub>		NdCo <sub>5</sub> $c$ (high $T$ ) Basal (low $T$ )	Nd <sub>2</sub> Fe <sub>17</sub> In plane
GdCo <sub>2</sub>	GdFe <sub>2</sub>	GdCo <sub>3</sub> $c$	GdFe <sub>3</sub>	Gd <sub>2</sub> Co <sub>7</sub> $c$	Gd <sub>6</sub> Fe <sub>23</sub>	GdCo <sub>5</sub> $c$	Gd <sub>2</sub> Fe <sub>17</sub> In plane
TbCo <sub>2</sub>	TbFe <sub>2</sub>	TbCo <sub>3</sub>	TbFe <sub>3</sub> In plane	Tb <sub>2</sub> Co <sub>7</sub>	Tb <sub>6</sub> Fe <sub>23</sub>	TbCo <sub>5</sub>	Tb <sub>2</sub> Fe <sub>17</sub> In plane
DyCo <sub>2</sub>	DyFe <sub>2</sub>	DyCo <sub>3</sub>	DyFe <sub>3</sub> In plane	Dy <sub>2</sub> Co <sub>7</sub>	Dy <sub>6</sub> Fe <sub>23</sub>	DyCo <sub>5</sub>	Dy <sub>2</sub> Fe <sub>17</sub> In plane

TABLE III. Influence of additive elements in amorphous  $R$ - $T$  films on perpendicular anisotropy, compensation, and Curie temperatures [ $T_{\text{comp}}$ : compensation temperature,  $T_C$ : Curie temperature,  $z$ : concentration of additive in at. %. The fifth column gives the concentration  $z_0$  for which  $K_u$  becomes zero at room temperature (RT)].

Element	Composition	$dT_{\text{comp}}/dz$	$dT_C/dz$	$K_u(\text{RT})=0$	Ref.
O	Gd <sub>24</sub> Tb <sub>4</sub> Fe <sub>72</sub>	-85	-10	2-4	30
O from H <sub>2</sub> O	Gd <sub>24</sub> Tb <sub>4</sub> Fe <sub>72</sub>	-120	-10	2.5	30
N	Gd <sub>26</sub> Fe <sub>74</sub>	-33 - -43	-10	7.5	30
N	Ge <sub>24</sub> Tb <sub>4</sub> Fe <sub>72</sub>	-35	-10	~8	30
N	Tb <sub>21</sub> Fe <sub>76</sub> Co <sub>3</sub>			4.4 <sup>a</sup>	31
N	Tb <sub>31</sub> Fe <sub>66</sub> Co <sub>3</sub>			2.8 <sup>a</sup>	31
Si, Ge	Gd <sub>26</sub> Fe <sub>74</sub>			≤ 5	32
Sn	Gd <sub>26</sub> Fe <sub>74</sub>	-24 <sup>b</sup>	-10	20	33,32
Bi	Gd <sub>26</sub> Fe <sub>74</sub>	-24 <sup>b</sup>	-12.5	~20	33,32
Pb	Gd <sub>26</sub> Fe <sub>74</sub>	-20 <sup>b</sup>	-14	~20	33
Au	Gd <sub>26</sub> Fe <sub>74</sub>	-15	-0.7	18	34
Al	Tb <sub>30</sub> Fe <sub>70</sub>			> 20	35
Be	TbFeCo		-5.6 <sup>c</sup>	> 40	36
Cr	Tb <sub>25</sub> Fe <sub>75</sub>		-13		
Cr	TbFeCo		-12.8	> 10 <sup>d</sup>	36

<sup>a</sup>Steep decrease to  $\frac{1}{4}$  of original value.

<sup>b</sup>Rough average, no linear dependence.

<sup>c</sup>For more than 6 at. %; for less no change is observed.

<sup>d</sup>For 10 at. % Cr in a TbFeCo disk a signal-to-noise ratio > 45 dB was obtained in recording experiments.

atively small shift, which has been attributed to an increase of the iron moment and a reduction of the exchange constants.<sup>33,37</sup> The effect on  $T_C$  is approximately the same for all additives (except for Be with its small atomic radius and for Au) and corresponds to a magnetic dilution, except for Au which is magnetically polarizable.

The effects of the reactive elements, especially of oxygen on  $K_u$ , are therefore much stronger than a "magnetic deactivation" of isolated  $R$  atoms could explain, in contrast to the effect on the magnetic system even if one assumes that, e.g., a divalent oxygen atom deactivates two  $R$  atoms. To our knowledge there has been no attempt in the literature to explain this drastic effect on  $K_u$ . In our model it is easily explained. A covalently bonded "molecule" will not just magnetically deactivate its "ligands," but will seriously deteriorate the hexagonal character of the local structural unit leading to a destruction of its perpendicular anisotropy.

Under the assumption that one additive atom "deactivates" 3-12  $R$  atoms and that this is due to a deterioration of the structural unit, we can estimate the size of the pseudocrystalline unit: it comprises typically 3-12 rare-earth atoms.

### C. Substrate temperature and annealing

The influence of substrate temperature during thin-film deposition by evaporation and annealing is shown in Fig. 4. In order to discuss the influence of crystallization, the corresponding temperature range up to 1100 K is also included.

In Tb<sub>31</sub>Fe<sub>69</sub> films prepared by flash evaporation a strong linear increase of the anisotropy constant with substrate temperature was found.<sup>38,46</sup> The same tendency has been observed for (Tb<sub>1-x</sub>Gd<sub>x</sub>)<sub>30</sub>Fe<sub>70</sub> thin films

(30-1060 nm thickness) prepared by flash evaporation of alloy powders.<sup>47</sup> Recently an increase of  $K_u$  for sputtered Tb<sub>1-x</sub>Fe<sub>x</sub> ( $x=0.62-0.75$ ) with increasing substrate temperature up to 670 K has been reported.<sup>4,19</sup>

For Nd<sub>35</sub>Fe<sub>65</sub> the situation is similar. In addition, above 540 K a rapid decrease of  $K_u$  to zero was observed and ascribed to crystallization of the amorphous film.<sup>39</sup>

Annealing experiments on Gd<sub>27</sub>Tb<sub>10</sub>Fe<sub>63</sub> films prepared by magnetron sputtering at 77 K have led to an increase

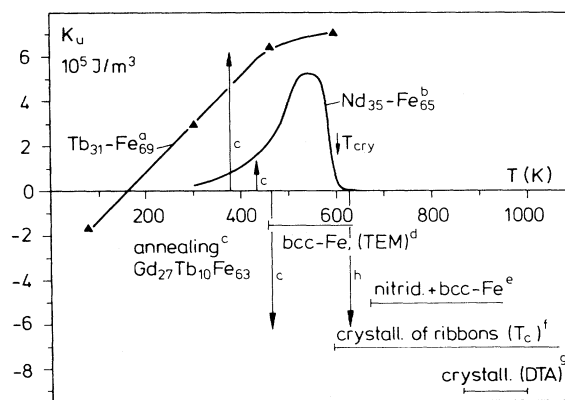


FIG. 4. Influence of substrate temperature and annealing on the perpendicular anisotropy of some amorphous  $R$ - $T$  films. Annealing effects on Gd<sub>27</sub>Tb<sub>10</sub>Fe<sub>63</sub> films prepared by magnetron sputtering at 77 K and with an initial  $K_u = 8 \times 10^4$  J/m<sup>3</sup> are indicated by vertical arrows. In the lower right part of the figure reported temperature ranges for crystallization are shown. The data have been taken from different references: <sup>a</sup>Ref. 38, <sup>b</sup>Ref. 39, <sup>c</sup>Ref. 40, <sup>d</sup>Refs. 41 and 42, <sup>e</sup>Ref. 12, <sup>f</sup>Ref. 43, <sup>g</sup>Ref. 44, <sup>h</sup>Refs. 4 and 45.

of  $K_u$  for an annealing temperature of 433 K but, at 463 K, to a continuous decrease.<sup>40</sup> These annealing effects are indicated in Fig. 4 by vertical arrows.

The increase of  $K_u$  with increasing substrate temperature and with annealing below 430 K for films deposited at 77 K is easily explained in our model: The hexagonal structures become more pronounced and the local environment approaches more the relaxed crystalline state. The decrease of  $K_u$  for annealing above 430 K cannot be explained with our model. However, this behavior can be attributed to undetected oxidation or nitrifying (see Sec. III D).

The occurrence of positive  $K_u$  for magnetron sputtering at 77 K, whereas for flash evaporation a negative  $K_u$  occurs, can be explained by the much higher energy of the particles in the sputtering process. In flash evaporation at low substrate temperature every atom should stick at the place where it arrives, resulting in an "ideal" amorphous structure. If energy is transferred to the growing film during deposition by bombarding the film surface with energetic species, the effective local surface temperature is elevated and site rearrangements can take place that for evaporation with low-energy species can occur only at higher substrate temperatures.

For films produced by magnetron sputtering or evaporation above room temperature, no significant increase of  $K_u$  after annealing has been observed but sometimes rather a slight decrease of about 10% in cases where protection measures against oxidation have been taken.<sup>48</sup> Effects of this order correspond to contaminations in the order of much less than 1 at. % and cannot, however, completely be ruled out. Even when excluding oxidation effects there is the possibility that annealing leads to a reduction of intrinsic stress (or stress-producing effects) and consequently to a reduction of the magnetoelastic contribution to anisotropy, which can be up to one-third of the total anisotropy.

Tb-Fe samples grown at 525 K (500 nm thick with  $K_u = 10^5 \text{ J/m}^3$ )<sup>4</sup>, and completely encapsulated in Nb (20 nm under, 30 nm over), with which Tb-Fe has been shown not to react, were annealed at 625 K for 2 h, causing  $K_u$  to drop to  $4 \times 10^4 \text{ J/m}^3$  (see Fig. 4).<sup>45</sup> In these samples oxidation or nitrifying can probably be ruled out. The annealing temperature is above the temperature where crystallization can occur, but no indications of nanocrystals are found so that this drop in  $K_u$  is probably a relaxation of the amorphous phase into a precrystalline state with more cubic local environments (see Sec. III D).

Considering all these effects, we conclude that films prepared by magnetron sputtering at lower sputter gas pressure or by vapor deposition at higher temperatures exhibit nearly the optimal pseudocrystalline structure.

#### D. Crystallization, oxidation, and nitrifying

For annealing temperatures above 450 K the presence of crystallites in the amorphous matrix has been reported.<sup>41,42,44</sup> The reported crystallization temperatures are given in Fig. 4. By heating UHV vapor-deposited amorphous samples of  $\text{Gd}_{23}\text{Fe}_{77}$  in a TEM it was found that the early stage of crystallization is characterized by the

formation of  $R$  oxide together with iron-rich nuclei<sup>49</sup> at temperatures starting above 410 K. In the following we discuss whether some of the observed annealing effects on  $K_u$  can be due to contamination or crystallization.

In annealing experiments with thin films it is very difficult to avoid oxidation or nitrifying originating from the substrate and from dielectric protective layers, typically nitrides or oxides. Extended x-ray-absorption fine structure (EXAFS) studies on cosputtered  $\text{Tb}_{20}\text{Fe}_{80}$  (100 nm thickness embedded in 70-nm thick  $\text{Si}_3\text{N}_4$ ) show that annealing at 670 K causes precipitation of bcc polycrystalline Fe.<sup>12</sup> Auger depth profiles on the same samples revealed a uniform presence of nitrogen in the bulk. Annealing at 470 K leads to a decrease in  $K_u$  but does not give rise to observable bcc Fe. Similar effects on  $K_u$  were obtained for  $\text{Gd}_{25}\text{Fe}_{75}$  covered by  $\text{SiO}_2$ :<sup>50</sup>  $K_u$  remains positive for a 1-h annealing up to 570 K and rapidly decreases to negative values at annealing above that temperature.

It is known that the addition of oxygen or nitrogen in small quantities reduces  $K_u$  drastically (see Sec. III B above). There are only a few experiments where it could be differentiated between oxidation and pure structural effects. For annealing experiments,<sup>48</sup>  $\text{Gd}_{17.5}\text{Tb}_{6.5}\text{Fe}_{76}$  specimens of different thickness up to  $0.5 \mu\text{m}$  were prepared by electron-beam evaporation at room temperature and covered by 50 nm protection layers of aluminum so that the data could be extrapolated to "infinite" thickness and therefore a distinction between surface and volume effects could be made. Structural relaxation processes up to 620 K mainly affected  $H_c$  while  $K_u$ ,  $M_s$ , and  $T_C$  remained nearly constant. For "infinitely" thick layers annealing below 420 K does not lead to a decrease in  $K_u$  but rather to a small increase,<sup>48</sup> for an annealing temperature of 520 K a decrease of  $K_u$  by 22% (Ref. 51) has been reported.

We therefore conclude that the sometimes observed strong decrease of  $K_u$  with annealing above 420 K (see Fig. 4) is caused by oxidation or nitrifying from the substrate or from dielectric protective layers.

The crystallization behavior of Gd-Fe was also determined by identification of Curie temperatures on 20- $\mu\text{m}$  thick ribbons of melt-spun amorphous Gd-Fe, with a Gd content between 22 and 70 at. %.<sup>43</sup> Although no statements about protection measures have been made, the influence of oxidation in these experiments was supposed to be largely reduced because of the thickness of the specimens. For all Gd concentrations  $\text{GdFe}_2$  (cubic, see Fig. 2) and bcc Fe were found, for  $T$ -rich compositions also  $\text{Fe}_{23}\text{Gd}_6$ . The crystallization temperature range extends from 570 to 1070 K.

Differential calorimetry of 1- $\mu\text{m}$  thick GdTb-Fe in an Ar atmosphere showed, however, that crystallization with measurable heat production starts at about 800 K.<sup>44</sup> In the presence of oxygen a process between 520 and 720 K is observed. It is therefore possible that even for the thick ribbons it is an oxidation of the rare-earth components that causes the beginning of precipitation of bcc Fe probably from the surface.

High-resolution electron microscopy has revealed the presence of small Fe or Co crystals (2.5–7 nm in diame-

ter) in unannealed 20-nm thick Tb-FeCo films.<sup>41</sup> Upon annealing for 36 h at 470 K the crystal size increased to up to 30 nm, but extensive areas remained amorphous.<sup>42</sup> The authors rule out the possibility of oxidation from the air because the films were encapsulated in 8–12-nm thick  $\text{Si}_3\text{N}_4$  layers. From the discussion above we suggest that at 470 K a diffusion of N into the *R-T* layer begins. In any case it is probable that a certain nitrifying of the *R-T* layer occurs during the reactive deposition of  $\text{Si}_3\text{N}_4$ . We therefore suppose that the precipitation of bcc Fe in TEM observations at temperatures below 600 K is an indirect effect of oxidation or nitrifying.

Assessing the annealing experiments altogether, we feel that the primary process between 450 and 600 K is oxidation or nitrifying from oxide or nitride protection layers leading to the precipitation of TEM-observable bcc Fe and to a decrease in  $K_u$ .

The result of this discussion relevant for the interpretation of Fig. 4 is that only the increase of  $K_u$  for an annealing below 400 K can be attributed to a structural change in the amorphous state, while at higher temperatures strong oxidation or nitrifying effects play a major role under the usual experimental conditions. At about 600 K crystallization begins. For Gd- and Tb-based alloys this leads to a formation of cubic environments and bcc Fe. For Nd-based alloys, which have no cubic intermetallics, corresponding experimental data are not yet available.

### E. Bombardment effects

Figure 5 shows the dependence of the density  $\rho$  (Ref. 51) and the perpendicular anisotropy constant  $K_u$  (Ref. 44) on the argon pressure  $p_{\text{Ar}}$  of magnetron-sputtered GdTb-Fe (target-substrate distance 6 cm).

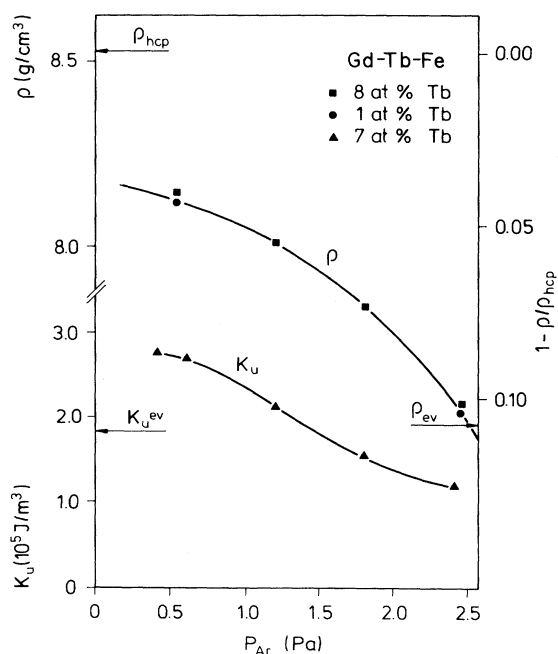


FIG. 5. Density  $\rho$  (Ref. 48) and uniaxial anisotropy constant  $K_u$  (Ref. 44) in dependence on sputter gas pressure.

Films sputtered at lower Ar pressures are generally denser and exhibit a higher  $K_u$ . At lower pressures the Ar atoms suffer fewer collisions before they hit the growing layer and therefore transfer more energy to its surface. The curve in Fig. 5 reaches a plateau for small  $p_{\text{Ar}}$ , in other work<sup>52,53</sup> (target-substrate distance not reported) a decrease in  $K_u$  for increasing and decreasing  $p_{\text{Ar}}$  with a maximum at about 1 Pa for  $\text{Tb}_{27}\text{Fe}_{73}$  and at about 1.3 Pa for  $\text{Tb}_{21}\text{Co}_{79}$  has been reported for films prepared by rf sputtering with zero substrate bias voltage.

Generally, evaporated films exhibit smaller anisotropies similar to those sputtered at higher Argon pressures.

Bias sputter deposition generally shows the trend of increasing anisotropy constant at increasing bias voltage. The results of different investigators differ in detail,<sup>54–56</sup> but typically a maximum in the range 100–200 V is obtained.

The tendency presented above is confirmed: Energy transfer to the growing film (here due to bombardment by ions accelerated by the substrate bias voltage) leads to an enhanced surface temperature and an increase in  $K_u$ . This effect on  $K_u$  can be explained in the same way as was done for the substrate temperature by a more pronounced pseudocrystalline structure. At very high energy transfer (high bias voltage, very low Ar pressure) a counter effect is observed, which can be understood as a destruction of the anisotropic structures by bombardment.

### F. Summary of experimental trends

Every measure that enables the amorphous structure to approach the energetically more favorable pseudocrystalline structure should enhance the magnetic anisotropy. The higher the energy in the growing layer, the more perfect, in the sense of our model, will the local environment be. This explains the increase of  $K_u$  with increasing substrate temperature or increasing energy due to additional ion bombardment.

An intrinsic crystallization (not generated by oxidation) or at least a precursor of crystallization with the formation of cubic environments begins at about 600 K and a decrease of  $K_u$  after annealing in that temperature region can be attributed to this effect. Annealing tends to increase  $K_u$ . This statement needs, however, more experimental examination. Drastic negative effects and crystallization below 600 K are probably primarily caused by oxidation or nitrifying.

One additive atom with covalent bonding destroys the anisotropy of structures comprising about six *R* atoms.

A maximum of  $K_u$  for compositions corresponding to  $RT_3$  is observed for amorphous Co-based amorphous alloys, whereas the situation for Fe-based films is less clear, and especially for the light *R*-Fe compounds (see Nd-Fe in Fig. 1) no maximum directly related to the composition occurs. As a generalized rule we find that decreases in  $K_u$  at certain compositions on the *R*-rich side are related to the occurrence of cubic intermetallics in the crystalline state.

#### IV. COMPARISON WITH EXISTING ANISOTROPY MODELS

##### A. General

For the development of a structural deviation from the ideal amorphous structure several mechanisms have been proposed.

A connection of positive  $K_u$  values to microcrystals in the amorphous films related to the intermetallic compounds  $R_2Fe_{17}$  to  $RFe_2$  was deduced from the occurrence of a  $K_u$  maximum for 15–30 at. %  $R$  atoms and an increase of  $K_u$  with substrate temperature for flash-evaporated TbGd-Fe films.<sup>57</sup> No connection of crystal orientation to the film plane was made. Fe-based intermetallics exhibit, however, in-plane anisotropy.  $RT_2$  compounds are cubic and corresponding environments in the amorphous state are, in our model, related to a decrease of perpendicular anisotropy.

One of the first mechanisms proposed was selective resputtering resulting in an anisotropic arrangement of nearest neighbors with a denser packing in the film plane compared to planes perpendicular to the surface.<sup>58</sup> Recently it was suggested that during growth an in-plane compressive stress due to implantation effects is introduced leading to a bond-orientational anisotropy<sup>3</sup> (see Sec. IV B). Both explanations do not hold for evaporated films.

In our model resputtering can be helpful to build the pseudocrystalline structures. It is, however, not the primary mechanism because the same magnitude of  $K_u$  can be obtained by evaporation at higher substrate temperatures. At too-high ion energies during sputter deposition, the pseudocrystalline structures can even be destroyed by bombardment (see Sec. III E).

Shape anisotropy from a columnar structure or a phase segregation combined with the columnar structure was discussed as a source of perpendicular anisotropy in amorphous Gd-Co.<sup>59</sup> However, a considerable perpendicular anisotropy is also found in thin films which show very little of these macroscopic inhomogeneities. On the contrary, it could be shown that the anisotropy increases when the columnar structure becomes less pronounced (see Fig. 5). We therefore expect diminishing contributions to the magnetic anisotropy from “columnar” or phase segregation effects compared to single-ion anisotropies in homogeneous Tb-rich films.

Magnetostrictive effects can contribute to the anisotropy; the magnetostrictive constant is positive.<sup>60</sup> They are, however, much smaller than single-ion anisotropies, but sometimes reach values of one-third of the total anisotropy.<sup>56,61,62</sup> A perpendicular magnetic anisotropy is found independent of stress. This confirms that magnetostrictive effects are not the primary mechanism. In any case magnetostriction is a continuous description. In our explanation of anisotropy we are looking for structural units which in themselves provide a structural anisotropy that can be enhanced by stress.

##### B. Bond-orientational anisotropy

When there is no macroscopic structural anisotropy, the only remaining anisotropy is one on an atomic scale. Small-angle x-ray scattering indicated indeed a larger mean nearest-neighbor distance perpendicular to the

plane compared to the same parameter in-plane corresponding to a strain of about 2.5%.<sup>3</sup> The authors call this structural anisotropy BOA (bond-orientational anisotropy). BOA was originally proposed for amorphous alloys when they are subjected to mechanical creep deformation.<sup>63</sup> This anelastic mechanism invokes the anisotropic distribution of the orientation of atomic pairs regardless of chemical identity.

A complete comparison with our model is not possible because, with BOA, so far no attempt has been made to explain all features of  $K_u$  as described in Sec. III, especially the compositional dependence and the destruction by additives.

BOA is a statistical description of the amorphous state without reference to an ordered atomistic structure. From such a general model of the structural anisotropy one expects that deposition at higher substrate temperatures and annealing leads to a decrease of  $K_u$  in contradiction to experimental results. There is also no significant effect on the anisotropy of stress during the deposition, and hence anelastic strain cannot be its origin.<sup>4</sup>

The experimental method seems to be very valuable and could be used to investigate structural changes related, e.g., to different compositions and to additives.

##### C. Precipitates and growth-induced texturing

In an attempt to explain the decrease of  $K_u$  at special compositions for cosputtered Tb-Fe by phase segregations, one suggestion was that precipitates of diameter less than 2 nm occur as a precursor to the formation of intermetallic (cubic)  $Tb_6Fe_{23}$ .<sup>64</sup> Our model explains the decrease of  $K_u$  on the  $R$ -rich side in a similar manner. It proposes, however, a more explicit environmental structure and applies more generally to the whole compositional range and to different binary systems.

In the growth-induced texturing model the structural anisotropy has been attributed to a texturing of the amorphous structure, which lowers the surface energy during growth analogous to texturing of the crystallographic orientation of vapor-deposited crystalline films.<sup>4</sup> The effect of deposition temperature is regarded to allow rearrangements of local structural units into energetically favorable orientations.

This model bears in more general terms a certain resemblance to our pseudocrystalline model, the preferential perpendicular orientation of which of the local environments during layer-by-layer growth can be regarded as a sort of “texturing.” Also the thermodynamical aspects are very similar, whereas the influence of composition and additives on  $K_u$  is not interpreted in the texturing model.

##### D. Anisotropic pair ordering

Very recently clear evidence for structural anisotropy in amorphous sputtered Tb-Fe has been obtained using x-ray-absorption fine-structure measurements.<sup>65</sup> Perpendicular anisotropy in these films is associated with Fe-Fe and Tb-Tb pair correlations which are greater in-plane and Tb-Fe correlations which are greater perpendicular to the film plane. These findings indicate local atom symmetries common to crystalline compounds and are con-

sistent with our layered model.

No structure is resolved beyond the near-neighbor peak indicating a lack of sharply defined interatomic distances beyond the nearest neighbors, and it can be stated with confidence that no ordering exists beyond the second neighbors ( $> 4 \text{ \AA}$ ).

Using EXAFS it is very difficult to obtain information on local bond angles and in the case of amorphous materials it is nearly impossible.<sup>66</sup> It is therefore not possible to get experimental evidence on whether a hexagonal-like type of ordering exists in the plane.

In Sec. III B we deduced that the formation of one "molecule" of  $R$  and a reactive element destroyed the anisotropy correlated with 3–12  $R$  atoms. This is more than the coordination number for  $R$ - $R$  neighbors (which is 0–4, see Table I), so that a certain type of clustering extending beyond the nearest neighbors, not necessarily an ordering with sharply defined interatomic distances, should exist.

## V. CONCLUSIONS

We developed a pseudocrystalline model for the magnetic anisotropy in amorphous thin  $R$ - $T$  films which is guided by the crystalline structure of  $R$ - $T$  intermetallics. The local structural units which are regarded as a model of the short-range order in the amorphous phase are estimated to comprise typically 6–12  $R$  atoms and are oriented in the layer-by-layer growth of the thin film. This size is estimated from the destruction of  $K_u$  by only 1–8 at. % "reactive" additives, which does not necessarily involve an ordering with sharply defined interatomic distances.

Our model is idealized. In reality the hexagonal units may not really homogeneously be formed, but a tendency toward formation is supported by the energetically minimal configuration in the crystalline structure and the layer by layer growth. The pseudocrystallinity is supposed to be a purely local structural effect and not viewed as truly nanocrystalline. It reflects the idea that the local atom symmetries in the amorphous state are similar to those of the crystalline counterparts.

It is assumed that the  $T$  atoms in the  $T$  plane relax in the amorphous state with respect to their crystalline positions, making crystalline second-nearest to nearest neighbors in the amorphous structure. With this relaxation, coordination numbers in accordance with experimental results are obtained.

The uniaxial magnetic anisotropy observed also in Fe-based amorphous alloys in contrast to their crystalline counterparts is assumed to be caused via spin-orbit coupling by axial local electrostatic fields with an average component parallel to the film normal at the  $R$  sites, which in turn are produced by the  $T$ -plane relaxation.

There is no direct evidence for this model, but it has all

the necessary features to explain qualitatively the major experimental trends, especially the increases of  $K_u$  with substrate temperature and annealing below 450 K, and the destruction of  $K_u$  by only 1–2 at. % oxygen. Annealing above about 600 K leads probably to crystallization or a precursor of crystallization with the formation of cubic environments in systems with cubic intermetallics in the corresponding compositional range. Consistent with our model this leads to a corresponding decrease of  $K_u$ . In order to further clarify this point more annealing experiments are necessary, carefully excluding the influence of oxygen and nitrogen on crystallization and anisotropy. The link of the amorphous to the crystalline state is most obvious in the compositional dependence of the anisotropy. The decrease of  $K_u$  on the  $R$ -rich side beyond  $RT_2$ , observed for all considered systems except Nd-Fe, is attributed to a tendency to form cubic environments in the amorphous state corresponding to the occurrence of cubic structures in the crystalline state, respectively to the absence of cubic structures in the crystalline Nd-Fe system.

For further experiments we recommend to observe the following precautions. In order to exclude oxidation and nitrifying effects, an extrapolation to infinite thickness should be done by measuring samples with different thickness. For handling the specimens at temperatures above 400 K they should be encapsulated in metallic layers, e.g., Al, Ti, or Nb and not in AlN, Si<sub>3</sub>N<sub>4</sub>, or SiO. In order to exclude an influence of  $T_C$  variations on  $K_u$  the measurements should be performed at low temperatures.

The best suited system seems to be Dy-T because of the strong spin-orbit coupling of Dy, on the one hand (advantage over Gd-based systems), and their relatively low coercive energy enabling measurements at low temperatures on the other hand (advantage over Tb-based systems). Co-based systems allow direct study of compositional and structural effects also on the  $T$ -rich side.

Recommended experiments to check our model would be to perform structural investigations (e.g., x-ray small-angle scattering or EXAFS) on films with compositions corresponding to maximum and zero  $K_u$ , evaporated at low and high temperatures, e.g., at 77 and at 300 K, and for films with maximum  $K_u$  compositions with 5 at. % covalent elements, as, e.g., Si or Ge or with 2 at. % oxygen. More work concerning the different behavior of Nd-Fe in comparison to the other binary alloys and more careful annealing experiments seem promising.

## ACKNOWLEDGMENTS

We gratefully acknowledge the discussions with K. H. J. Buschow, A. M. J. Spruijt, F. J. A. den Broeder, A. G. Dirks, and J. P. Krumme of Philips Research and Development.

<sup>1</sup>J. Orehtsky and K. Schröder, *J. Appl. Phys.* **43**, 2413 (1972).

<sup>2</sup>P. Chaudhari, J. J. Cuomo, and R. J. Gambino, *Appl. Phys. Lett.* **22**, 337 (1973).

<sup>3</sup>X. Yan, M. Hirscher, T. Egami, and E. E. Marinero, *Phys. Rev. B* **43**, 9300 (1991).

<sup>4</sup>F. Hellman and E. M. Gyorgy, *Phys. Rev. Lett.* **68**, 1391

(1992).

<sup>5</sup>R. Sato, N. Saito, and Y. Togami, *Jpn. J. Appl. Phys.* **24**, L266 (1985).

<sup>6</sup>R. C. O'Handley, *J. Appl. Phys.* **62**, R15 (1987).

<sup>7</sup>D. T. Cromer, A. C. Larson, *Acta Crystallogr.* **12**, 855 (1959).

<sup>8</sup>G. F. Bertaut, R. Lemaire, and J. Schweizer, *C. R. Acad. Sci.*

- 260, 3595 (1965).
- <sup>9</sup>K. H. J. Buschow, Rep. Prog. Phys. **40**, 1179 (1977).
- <sup>10</sup>K. Fukuda, S. Katayama, T. Katayama, A. Nukui, and A. Makisima, Jpn. J. Appl. Phys. **25**, 1640 (1986).
- <sup>11</sup>Y. Kato, S. Takayama, E. Matsubara, and Y. Waseda, Jpn. J. Appl. Phys. **30**, 764 (1991).
- <sup>12</sup>C. J. Robinson, M. G. Samant, and E. E. Marinero, Appl. Phys. A **49**, 619 (1989).
- <sup>13</sup>V. G. Harris, K. D. Aylesworth, K. H. Kim, W. T. Elam, and N. C. Koon, J. Appl. Phys. **70**, 6311 (1991).
- <sup>14</sup>H. J. Leamy, G. H. Gilmer, and A. G. Dirks, in *Current Topics in Materials Science*, edited by E. Kaldis (North-Holland, Amsterdam, 1980), Vol. 6, p. 309.
- <sup>15</sup>V. G. Harris, K. D. Aylesworth, B. N. Das, W. T. Elam, and N. C. Koon, IEEE Trans. Magn. **20**, 2958 (1992).
- <sup>16</sup>T. Miyazaki, K. Hayashi, S. Yamaguchi, M. Takahashi, A. Yoshihara, T. Shimamori, and T. Wakiyama, J. Magn. Mater. **75**, 243 (1988).
- <sup>17</sup>M. Takahashi, A. Yoshihara, T. Shimamori, T. Wakiyama, T. Miyazaki, K. Hayashi, and S. Yamaguchi, J. Magn. Mater. **75**, 252 (1988).
- <sup>18</sup>M. Takahashi, T. Shimamori, T. Miyazaki, T. Wakiyama, and A. Yoshihara, IEEE Trans. J. Magn. Jpn. **4**, 666 (1989).
- <sup>19</sup>R. B. van Dover, M. Hong, E. M. Gyorgy, J. F. Dillon Jr., and S. D. Alibiston, J. Appl. Phys. **57**, 3897 (1985).
- <sup>20</sup>T. Suzuki, Jpn. J. Appl. Phys. **24**, L199 (1985).
- <sup>21</sup>R. G. Taylor, T. R. McGuire, J. M. D. Coey, and A. Gangulee, J. Appl. Phys. **49**, 2885 (1978).
- <sup>22</sup>M. Takahashi, T. Shimamori, T. Miyazaki, K. Hayashi, and T. Wakiyama, IEEE Trans. Magn. **MAG-23**, 3314 (1987).
- <sup>23</sup>F. Hellman, R. B. van Dover, S. Nakahara, and E. M. Gyorgy, Phys. Rev. B **39**, 10591 (1989).
- <sup>24</sup>P. Hansen, C. Clausen, G. Much, M. Rosenkranz, and K. Witter, J. Appl. Phys. **66**, 756 (1989); P. Hansen, S. Klahn, C. Clausen, G. Much, and K. Witter, *ibid.* **69**, 3194 (1991).
- <sup>25</sup>T. Katayama and T. Shibata, J. Magn. Mater. **23**, 173 (1981).
- <sup>26</sup>N. Sato, J. Appl. Phys. **59**, 2514 (1986).
- <sup>27</sup>Z. S. Shan, D. J. Sellmyer, S. S. Jaswal, Y. J. Wang, and J. X. Shen, Phys. Rev. Lett. **63**, 449 (1989).
- <sup>28</sup>Z. S. Shan and D. J. Sellmyer, Phys. Rev. B **42**, 10433 (1990).
- <sup>29</sup>Z. S. Shan, D. J. Sellmyer, S. S. Jaswal, Y. J. Wang, and J. X. Shen, Phys. Rev. B **42**, 10466 (1990).
- <sup>30</sup>H. Heitmann, A. M. J. Spruijt, P. Willich, and H. Wilting, J. Appl. Phys. **61**, 3343 (1987).
- <sup>31</sup>S. Hashimoto, Y. Ochiai, and M. Kaneko, IEEE Trans. Magn. **MAG-23**, 2278 (1987).
- <sup>32</sup>M. Hartmann, K. Witter, and P. Willich, IEEE Trans. Magn. **MAG-21**, 2044 (1985).
- <sup>33</sup>M. Hartmann, P. Hansen, and P. Willich, J. Appl. Phys. **56**, 2870 (1984).
- <sup>34</sup>P. Hansen and M. Hartmann, J. Appl. Phys. **59**, 859 (1986).
- <sup>35</sup>K. Aratani, T. Kobayashi, S. Tsunishima, and S. Uchiyama, J. Appl. Phys. **57**, 3903 (1985).
- <sup>36</sup>N. Horiai, T. Ohashi, S. Yoshida, M. Miura, T. Tokushima, and T. Fujii, J. Appl. Phys. **69**, 4764 (1991).
- <sup>37</sup>P. Hansen and M. Urner-Wille, J. Appl. Phys. **50**, 7471 (1979).
- <sup>38</sup>Y. Takeno, M. Suwabe, T. Sakurai, and K. Goto, Jpn. J. Appl. Phys. **25**, L657 (1986).
- <sup>39</sup>T. Suzuki, A. Murakami, T. Katayama, IEEE Trans. Magn. **MAG-23**, 2958 (1987).
- <sup>40</sup>Y. J. Wang, H. Cai, Q. Tang, K. M. Yang, J. Y. Li, and J. L. Wang, J. Magn. Mater. **66**, 84 (1987).
- <sup>41</sup>Z. G. Li and D. J. Smith, Appl. Phys. Lett. **55**, 919 (1989).
- <sup>42</sup>Z. G. Li, D. J. Smith, E. E. Marinero, and J. A. Willett, J. Appl. Phys. **69**, 6590 (1991).
- <sup>43</sup>K. Yano, K. Tokumitsu, E. Kita, H. Ino, and A. Tasaki, Jpn. J. Appl. Phys. **30**, L482 (1991).
- <sup>44</sup>S. Klahn, dissertation, Universität Hamburg, Germany, 1990.
- <sup>45</sup>F. Hellman (private communication).
- <sup>46</sup>Y. Takeno, M. Suwabe, and K. Goto, IEEE Trans. Magn., **MAG-23**, 2141 (1987).
- <sup>47</sup>Y. Takeno, K. Kaneko, and K. Goto, Jpn. J. Appl. Phys. **30**, 1701 (1991).
- <sup>48</sup>S. Klahn, M. Hartmann, K. Witter, and H. Heitmann, in *Magnetic Properties of Amorphous Metals*, edited by A. Hernandez, V. Madurga, M. C. Sanchez-Trujillo, and M. Vazquez (Elsevier, New York, 1987), p. 176.
- <sup>49</sup>A. G. Dirks and J. R. M. Gijbers, Thin Solid Films **58**, 333 (1979).
- <sup>50</sup>S. Tsunashima, T. Shinoda, H. Miyatake, and S. Uchiyama, J. Appl. Phys. **51**, 5901 (1980).
- <sup>51</sup>S. Klahn, H. Bentin, B. Knörr, H. Heitmann, and H. Wilting, J. Appl. Phys. **67**, 1442 (1990).
- <sup>52</sup>M. Ohkoshi, M. Harada, T. Tokunaga, S. Honda, and T. Kusuda, IEEE Trans. Magn. **MAG-21**, 1635 (1985).
- <sup>53</sup>S. Ohbayashi, M. Harada, M. Nawate, M. Ohkoshi, S. Honda, and T. Kusuda, IEEE Trans. J. Magn. Jpn. **TJMJ-2**, 340 (1987).
- <sup>54</sup>S. Takayama, T. Niihara, K. Kaneko, Y. Sugita, and M. Ojima, J. Appl. Phys. **61**, 2610 (1987).
- <sup>55</sup>D. D. Bacon, M. Hong, E. M. Gyorgy, P. K. Gallagher, S. Nakahara, and L. C. Feldman, Appl. Phys. Lett. **48**, 730 (1986).
- <sup>56</sup>T. Kusuda, S. Honda, and M. Ohkoshi, J. Appl. Phys. **53**, 2338 (1982).
- <sup>57</sup>Y. Takeno, K. Kaneko, and K. Goto, J. Magn. Soc. Jpn. **15**, S1, 201 (1991).
- <sup>58</sup>R. J. Gambino and J. J. Cuomo, J. Vac. Sci. Technol. **15**, 296 (1978).
- <sup>59</sup>S. R. Herd, J. Appl. Phys. **49**, 1744 (1978).
- <sup>60</sup>D. W. Forester, C. Vittoria, J. Schelleng, and P. Lubitz, J. Appl. Phys. **49**, 1966 (1978).
- <sup>61</sup>Y. Suzuki, S. Takayama, F. Kirino, and N. Ohta, IEEE Trans. Magn. **MAG-23**, 2275 (1987).
- <sup>62</sup>S. C. N. Cheng, M. H. Kryder, and M. C. A. Mathur, IEEE Trans. Magn. **25**, 4018 (1989).
- <sup>63</sup>Y. Suzuki, J. Haimovich, and T. Egami, Phys. Rev. B **35**, 2162 (1987).
- <sup>64</sup>F. Hellman, R. B. van Dover, and E. M. Gyorgy, Appl. Phys. Lett. **50**, 296 (1987).
- <sup>65</sup>V. G. Harris, K. D. Aylesworth, B. N. Das, W. T. Elam, and N. C. Koon, Phys. Rev. Lett. **69**, 1939 (1992).
- <sup>66</sup>V. G. Harris (private communication).